International Journal of Engineering and Technical Research (IJETR)
ISSN: 2321-0869, Volume-2, Issue-4, April 2014

Study of nanocrystalline structure and micro properties of ZnO powders by using Rietveld method

Tagreed. M. Al-Saadi, Nabeel A. Bakr, Noor A. Hameed

***Abstract*— In this study, we report the qualitative phase analysis performed by Rietveld X-ray diffraction using "Fullprof" program for two different samples of ZnO before and after heat treatment at (1200 °C). Two samples under study, first is a nanopowder, second is a micropowder. Rietveld refinement on X-ray data for the samples is performed. The obtained results have a good optimization between the observed X-ray diffraction patterns and that calculated by Rietveld analysis. This optimization is determined according to R_p, R_{wp} and GOF. The lattice parameters, space group and other structural factors were calculated. The particle morphology of the powder before and after heat treatment were identified using SEM. The final result shows that Rietveld refinement give exact results compared to other known methods for the study of the structural properties.**

***Index Terms*— Rietveld method, Qualitative analysis, Fullprof, XRD, ZnO powder.**

I. INTRODUCTION

Zinc oxide is an inorganic compound with the formula ZnO. It usually appears as a white powder, nearly insoluble in water. The powder is widely used as an additive into numerous materials and products including plastics, ceramics, glass, cement, rubber and lubricants [1]. Zinc oxide crystallizes in three forms [2]: hexagonal wurtzite, cubic zinc blende and cubic rock salt. At ambient pressure and temperature, ZnO crystallizes in the wurtzite structure. It has a hexagonal lattice, characterized by two interpenetrating hexagonal close packed (hcp) sublattices of Zn^{+2} and O^{-2}, with lattice spacing a = 0.325 nm and c = 0.521 nm and space group $P6_3mc$. The lattice parameters of the unit cell have a c/a ratio of (1.602) which is 1.8 % off of the ideal hexagonal-close-packed structure of (1.633)[3-7].

II. EXPERIMENTAL WORK

A. Materials

The structure investigations were performed on two commercial zinc oxide materials:

Commercial nanopowder (Hongwu Nanometer Co. Ltd., Reagent Grade, 40-50 nm, 99.9% purity).

Commercial micropowder (Hongwu Nanometer Co. Ltd., Reagent Grade, 70-80 nm, 99.9% purity).

B. Experimental Conditions

The collection of X-ray diffraction patterns s was performed by the use (Shimadzu XRD-6000) goniometer using copper target (Cu K_α, 1.5406 Å), (40 kV, 30 mA). The samples were mounted in an aluminum sample holder. Step-scan data were collected from (20°-100°) with a step width of 0.02°. The time of data acquisition was chosen to obtain the intensity of the most intense diffraction line of 5 sec/step counts for all X-ray patterns s. The divergence, scattering, and receiving slits are 1.0◦, 1.0◦ and 0.30 (mm) respectively. The Rietveld analysis was performed applying Fullprof program.

C. Rietveld Analysis

Rietveld method can be defined is a crystal structure refinement method, from powder diffraction data. A patterns is calculated from a series of structural parameters (cell, atomic coordinates, thermal motion, etc) and peak shape and width parameters (plus background, Lorentz-polarisation correction, etc), and compared to the observed data [8, 9]. Rietveld method can be used to solve a structure from the powder diffraction data. It starts by taking a trial structure, calculating a powder diffraction profile from it and then comparing it with the measured profile. The trial structure can then be gradually modified by changing the atomic positions and refined until a best-fit match with the measured patterns is obtained. The validity of the structure obtained is assessed by an R factor, and by a difference plot of the two patterns s [10]. The basic idea behind the Rietveld method is the calculation of the entire powder patterns using a variety of different refinable parameters. The parameters can roughly be divided into three categories: structural parameters, which mainly affect the intensities of the Bragg reflections, profile parameters, which are determined by the instrument, the sample, and background parameters [11].

The Rietveld method uses a model to calculate diffraction pattern which is then compared with observed data. The difference between all data set points of the observed and the calculated profiles is minimized by a least squares refinement of selected parameters. The least-squares refinement leads to a minimal residual quantity S_y [12, 13]:

$$S_y = \sum_i w_i (Y_{oi} - Y_{ci})^2 \quad (1)$$

Where Y_{oi} : is the observed intensity at point i of the observed powder patterns , Y_{ci} : is the calculated intensity for the i_{th} data point and w_i : The weight at point *i* in the diffraction profile is based on the counting statistics.

Many different statistical agreement factors have been proposed for judging the quality of a Rietveld refinement. The most common one is the so called weighted profile R-factor (R_{wp}). That these factors measure not just how well the structural model fits the diffraction intensities, but also how well we have fit the background and how well the diffraction

Manuscript received April 18, 2014.

Tagreed. M. Al-Saadi, Department of Physics, College of Education for Pure Science, University of Baghdad, Baghdad, Iraq

Nabeel A. Bakr, Department of Physics, College of Science, University of Diyala, Diyala, Iraq .

Noor A. Hameed, Department of Physics, College of Science, University of Diyala, Diyala, Iraq .

positions and peak shapes have been fit[11, 14].

The calculated intensities y_{ci} are determined by summing the contributions from neighboring Bragg reflections plus the background [15, 16]:

$$Y_{ci} = S\sum_k L_k F_k Ø (2Θ_i - 2Θ_k) O_k A + Y_{bi} \quad (2)$$

Where S: is the scale factor, K : represents the Miller indices (hkl) for a Bragg's reflection (which depends on the: symmetry), L_k : is a function containing Lorentz, polarization and multiplicity factors, Ø : the reflection profile function, O_k : is the preferred orientation function, A : is an is an absorption correction factor. (which depends on the: thickness of the sample, diffraction geometry and actual weighted average linear absorption coefficient). It is constant throughout the patterns, and is normally included in the scale factor), $F_{k:}$ is the structure factor for (k^{th}) Bragg reflection and $Y_{bi:}$ is the background intensity at i^{th} step.

At the end of a refinement it is necessary to check whether the results are meaningful, and whether they meet certain standard criteria**.** Through measure the agreement between the observed and calculated models. One of the ways to measure the agreement between the observed and calculated models is adjust the various atomic parameters so that the calculated structure factors match the observed structure factors as closely as possible .The factors called (Reliability factors) sometimes called the agreement factors. There are several R values: R-structure factor (R_F), R-Bragg factor (R_B), R-patterns factor (R_p), the weighted-profile factor (R_{wp}) and the expected factor (R_{exp})[17, 18].

1. Weighted-profile Reliability factors [19, 20]

$$R_{wp} = \sum_i W_i (y_{oi} - y_{ci})^2 / \sum_i W_i (y_{oi})^2 \quad (3)$$

2. Expected Reliability factors [21]

$$R_{exp} = [(N - P) / \sum_i W_i (y_{oi})^2]^{1/2} \quad (4)$$

3. The goodness of fit (χ^2) [20, 22]

$$\chi = [S_y / (N\text{-}P)]^{1/2}$$

$$\chi^2 = \sum_i w_i (Y_{i-} Y_{ci})^2 / (N\text{-}P) = R_{wp} / R_{exp} \quad (5)$$

Where **N**: is the number of observations and P: is the number of parameters.

D. Williamson-Hall Method

Williamson-Hall method of the X-ray analysis for precise determination of crystallite size distribution and analysis of lattice strains [23].

The average crystalline size was calculated using Debye-Scherrer's formula [24-27]:

$$D = K\lambda / \beta_D \cos\Theta \quad (6)$$

where D : crystalline size, K : a constant whose value depends on particle shape, λ : wavelength of Cu kα radiation and β_D : is the broadening solely due to small crystallite size.

The strain induced in powders due to crystal imperfection and distortion was calculated using the formula:

$$\varepsilon = \beta_s / 4\tan\Theta \quad (7)$$

Where $\beta_{s.}$ is the peak broadening due to lattice strain, Θ: is the Bragg's angle.

From above two equations, it was confirmed that the peak width from crystallite size varies as 1/cosΘ strain varies as tanΘ. Assuming that the particle size and strain contributions to line broadening are independent to each other and both have a Cauchy-like profile, the total peak broadening β_{hkl} may be expressed as:

$$\beta_{hkl} = \beta_D + \beta_s \quad (8)$$

$$\beta_{hkl} \cos\Theta = (K\lambda / D) + (4\varepsilon \sin\Theta) \quad (9)$$

The above equations are W-H equations. A plot is drawn with sinΘ along the x-axis and β_{hkl} cosΘ along the y-axis.

III. RESULTS AND DISCUSION

XRD patterns s of all samples are shown in figures (1a, 1b, 1c, 1d).

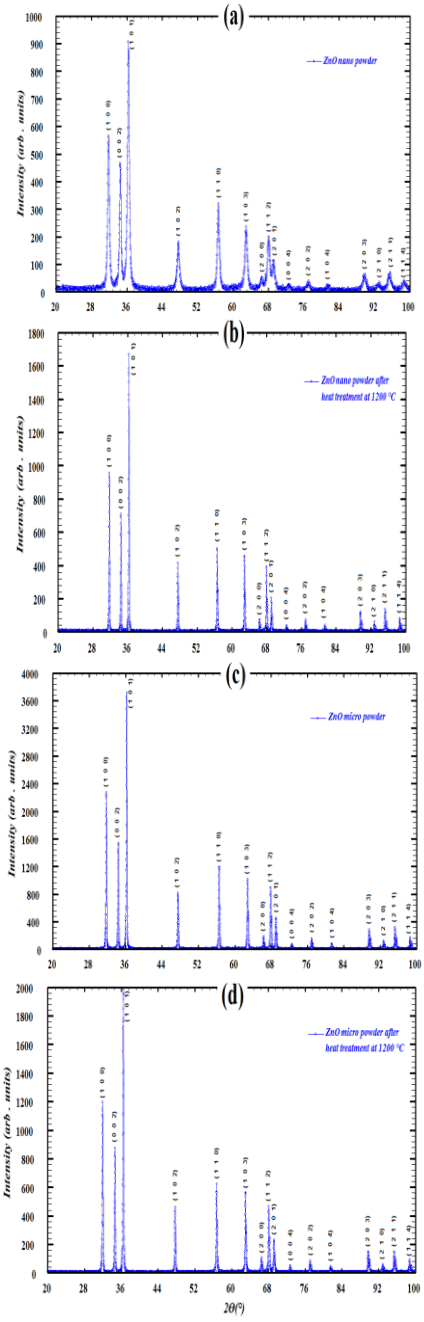

Fig. (1): X-ray diffraction patterns of: (a) ZnO nanopowder, (b) ZnO nanopowder after heat treatment at (1200 °C), (c) ZnO micropowder , (d) ZnO micropowder after heat treatment at (1200 °C).

The patterns s of ZnO nano powder before and after heat treatment at (1200 °C) exhibited strong diffraction peaks at (36.318°, 31.838°, 34.488°) and 36.310°, 31.826°, 34.487°) respectively. While XRD patterns s of ZnO micro powder before and after heat treatment at (1200 °C) exhibited strong diffraction peaks at (36.312°, 31.829°, 34.489°) and (36.457°, 31.972°, 34.640°) respectively.

Rietveld refinements of all samples ZnO are shown in Figure (2). The experimental points are plotted as dots (.) and theoretical data (calculated by equation 2) are shown as solid line. The difference between theoretical and experimental data is shown in the bottom line of each figure. The vertical lines represent the Bragg's allowed peaks.

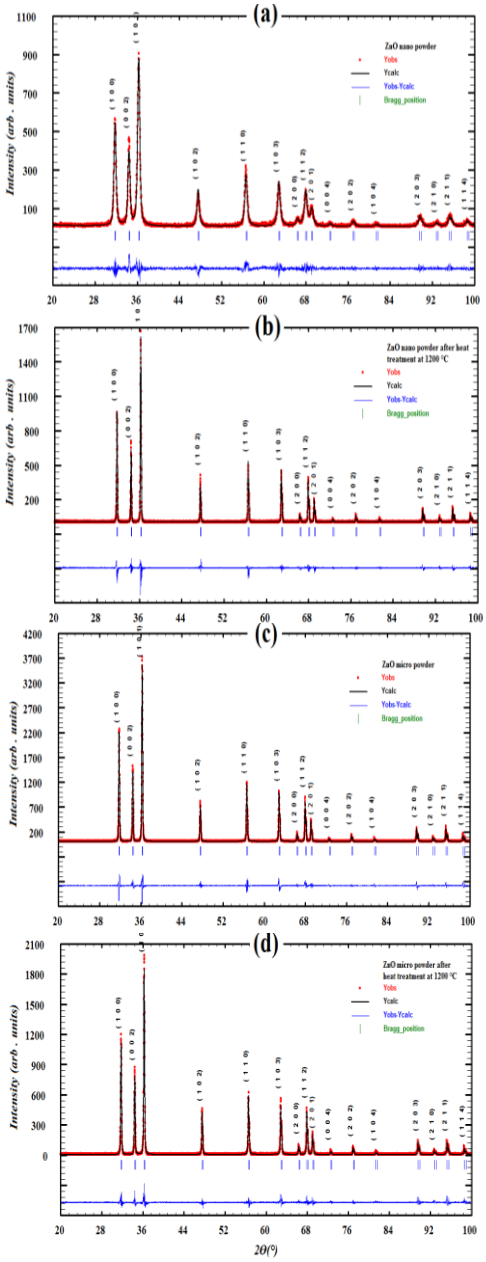

Fig. (2): The refined XRD patterns of ZnO (a) nanopowder, (b) nano powder before heat treatment, (c) micropowder,(d) micro powder after heat treatment. The red line is the experimental data; the blue line is the theoretical data. The lowest trace indicates the difference between patterns. The middle vertical lines indicate the peak position.

Table (1) shows unit cell parameters, crystal system, space group and unit cell volume for ZnO nano and micro powders before and after heat treatment.

Table (1): Unit cell parameters, crystal system, space group and unit cell volume for ZnO powders.

Samples ZnO powders	Heat treatment at	Unit cell parameters (Å)		Phase	Space group	Volume (Å^3)	$\frac{c}{a}$
		a=b	c				
nano	-	3.247	5.206	Hex.	P 6$_3$ m c	47.540	1.6021
nano	1200 °C	3.249	5.204	Hex.	P 6$_3$ m c	47.626	1.6015
micro	-	3.248	5.205	Hex.	P 6$_3$ m c	47.539	1.6014
micro	1200 °C	3.259	5.202	Hex.	P 6$_3$ m c	47.548	1.6013

Samples ZnO powders	Heat treatment at	D (W-H) nm	ε (W-H)*10^{-3}	D (Scherrer) nm
nano	-	17.33	-0.75	19.73
nano	1200 °C	19.88	-3	33.96
micro	-	46.21	-0.5	60.07
micro	1200 °C	69.32	-0.25	64.48

Table (2) shows strain and grain size according to Williamson-Hall and grain size according to Debye-Scherrer for ZnO nano and micro powders before and after heat treatment.

Table (2): Strain and grain size according to W-H and grain size according to Debye-Scherrer for ZnO powders.

From table (2) it is shown that the average grains sizes of the ZnO powders after heat treatment for both powders is increased. The difference between grain size according to W-H and grain size according to Debye-Scherrer occurs because W-H method takes into account the microstrain generated between atoms due to the defects and distortions in crystal. A negative value for the strain means lattice shrinkage.

The SEM micrographs for ZnO nano powder before and after heat treatment (Fig. 3a and 3b) show that a network formation and agglomeration has taken place. The SEM micrographs clearly show the microstructural homogeneity and remarkably dense mode of packing of grains of ZnO nanoparticles.

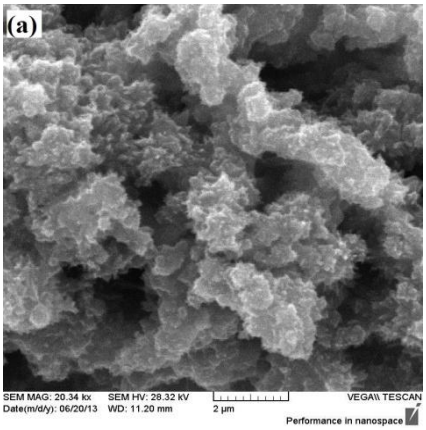

Fig. (3a): SEM images of ZnO nano powder before heat treatment.

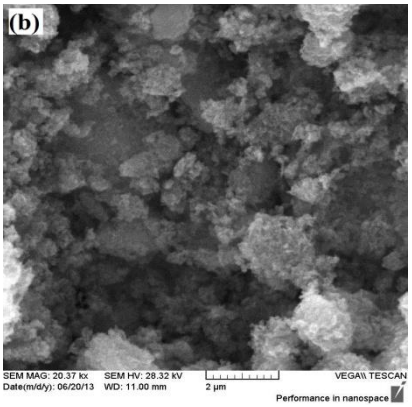

Fig. (3b): SEM images of ZnO nano powder after heat treatment.

The SEM micrographs for ZnO micro powder before heat treatment (Fig. 4a) show the particle that the columnar and polygon surface. After heat treatment SEM micrograph images (Fig. 4b) show the grains have pyramid forms.

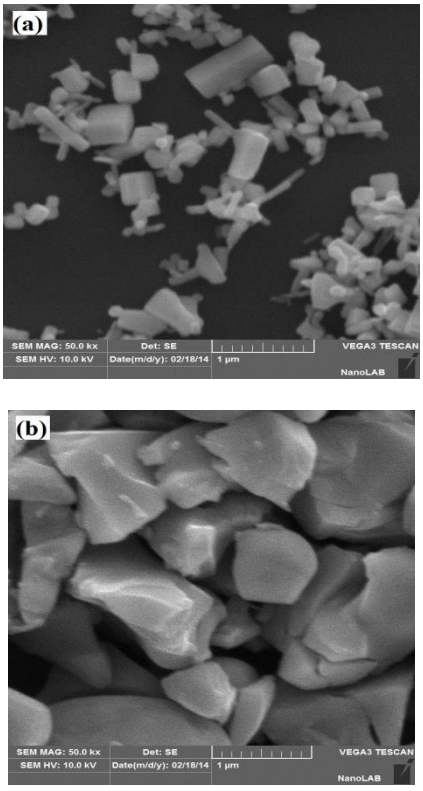

Fig. (4): SEM images of ZnO micro powder: (a) before heat treatment, (b) after heat treatment.

IV. CONCLUSIONS

Qualitative phase analysis performed by Rietveld X-ray diffraction using "Fullprof" program for nano and micro ZnO before and after heat treatment at (1200 °C). The obtained results showed a good agreement between the observed X-ray diffraction patterns and that the calculated by Rietveld technique. The results show that the grains size estimated by Debye-Scherrer formula and Williamson-Hall formula increases after heat treatment for both the nano and micro ZnO powder. No phase transition occurred because the powders need to heat treatment at high temperature. The SEM micrographs for ZnO nano powder show that a network formation and agglomeration has taken place. The SEM micrographs for ZnO micro powder before heat treatment show the particle that the columnar and polygon surface for after heat treatment SEM micrograph images show the grains have pyramid forms. The result shows that Rietveld refinement give exact results compared to other known methods for the study of the structural properties.

REFERENCES

[1] A. Hernandezbattez, R. Gonzalez, J. Viesca, J. Fernandez, J. Diazfernandez, A. MacHado, R. Chou and J. Riba, "CuO, ZrO_2 and ZnO nanoparticles as antiwear additive in oil lubricants" Wear, Vol. 265, P.422-428, (2008).
[2] A. Khan, "Synthesis, characterization and luminescence properties of znic oxide nanostructures", August, (2006).
[3] S. Baruah and J. Dutta, "Hydrothermal growth of ZnO nanostructures", Sci. Technol. Adv. Mater., Vol. 10, (2009).
[4] M´. M. Mas´ıs, "Fabrication and study of ZnO micro- and nanostructures" , (2007).
[5] C. Jagadish and S.J. Pearton, "Zinc Oxide Bulk, Thin Films and Nanostructures Processing, Properties, and Applications" (2006).
[6] C. Klingshirn, "ZnO: material, physics and applications", Chem Phys Chem, Vol. 8, p.p(782 – 803), (2007).
[7] Ü. Özgür, Y. I. Alivov, C. Liu, A. Teke, M. A. Reshchikov, S. Doğan, V. Avrutin, S.-J. Cho, H. Morkoç, S.- J. Cho, and H. Morkoçd, "A comprehensive review of ZnO materials and devices", Journal of Applied Physics, Vol. 98, (2005).
[8] H. M. Rietveld, "A profile refinement method for nuclear and magnetic structures" , J. Appl. Cryst., Vol. 2, p.p(65-71), (1969).
[9] H. M. Rietveld, "Line profiles of neutron powder-diffraction peaks for structure refinement", Acta Cryst., Vol. 22, p.p(151-152), (1967).
[10] L. E. Smart and E. A. Moore, "Solid state chemistry 3rd edition", Taylor & Francis group, LLC (2005).
[11] R. E. Dinnebier and K. Friese, "Modern xrd methods in mineralogy".
[12] K. Ståhl, "Powder diffraction and the Rietveld method", (2008).
[13] R. Snellings, L. Machiels, G. Mertens and J. Elsen "Rietveld refinement strategy for quantitative phase analysis of partially amorphous zeolitized tuffaceous rocks", Geologica belgica, Vol. 13, p.p(183-196), (2010).
[14] B. H. Toby, "R factors in Rietveld analysis: How good is good enough?", International Centre for Diffraction Data, Vol. 21, p.p(62-70), (2006).
[15] T. F. de Oliveira, R. R. de Avillez, E. K. Epprecht, J. C. B. Queiroz, " Evaluation via multivariate techniques of scale factor variability in the Rietveld method applied to quantitative phase analysis with X- ray powder diffraction", Materials research, Vol. 9, p.p(369-374), (2006).
[16] M. Karolus, "Aplications of Rietveld refinement in Fe-B-Nb alloy structure studies", Proceedings of the 12th scientific international conference "Achievements in mechanical and materials engineering", AMME'2003, Gliwice-Zakopane, p.p(723-726), (2003).
[17] G. Will, "Powder diffraction the Rietveld method and the two stage method to determine and refine crystal structures from powder diffraction data ", Springer, (2005).
[18] R. Saravanan and M. P. Rani, "Metal and alloy bonding - an experimental analysis", Springer, (2012).
[19] T. A. Al-Dhahir, "Quantitative phase analysis for titanium dioxide from X-ray powder diffraction data using the Rietveld method", Diyala journal for pure sciences, Vol. 9, p.p(108-119), (2013).
[20] L. B. Mccusker, R. B. Von Dreele, D. E. Cox, D. LoueËr and P. Scardi, "Rietveld refinement guidelines", J. appl. cryst., Vol.32, p.p(36-50), (1999).
[21] D. G. Porob and T. N. Guru row uru , "Ab initio structure determination via powder X-ray diffraction", Indian Academy of Sciences, Vol. 113, p.p(435–444), (2001).
[22] R. Nowosielski, R. Babilas, G. Dercz and L. Pająk , "Microstructure of polymer composite with barium ferrite powder", Journal of achievements in materials and manufacturing engineering, JAMME, Vol. 31, p.p(269-274), (2008).

[23] R. E. Goforth, K. T. Hartwig and L. R. Cornwell (auth.), T. C. Lowe, R. Z. Valiev (eds.), "Investigations and applications of severe plastic deformation", Springer-science and Business media dordrecht, (2000).
[24] VD Mote, Y. Purushotham and BN Dole, "Williamson-Hall analysis in estimation of lattice strain in nanometer-sized ZnO particles", Journal of Theoretical and Applied Physics, Vol. 6, p.p(1-8), (2012).
[25] A. K. Zak, W.H. Abd. Majid , M.E. Abrishami , R. Yousefi, "X-ray analysis of ZnO nanoparticles by Williamson-Hall and size-strain plot methods ", Solid State Sciences, Vol. 13, p.p(251-256), (2011).
[26] B. R Rehani, P B Joshi, K. N Lad and A. Pratap, "Crystallite size estimation of elemental and composite silver nano-powders using XRD principles", Indian Journal of Pure & Applied Physics, Vol. 44, p.p(157- 161), (2006).
[27] Y. T. Prabhu, K. V. Rao, V. S. Sai Kumar, B. S. Kumari, " X-ray analysis of Fe doped ZnO nanoparticles by Williamson-Hall and size-strain plot", International Journal of Engineering and Advanced Technology (IJEAT), Vol. 4, p.p(268-274), (2013).